Colloids and Surfaces B: Biointerfaces 230 (2023) 113486

Contents lists available at ScienceDirect

Colloids and Surfaces B: Biointerfaces

journal homepage: www.elsevier.com/locate/colsurfb

3D-printed biosurfactant-chitosan antibacterial coating for the prevention of silicone-based associated infections

Francisco Narciso [a,b], Sara Cardoso [a], Nuno Monge [c], Madalena Lourenço [a], Victor Martin [d,e], Noélia Duarte [a], Catarina Santos [f,g], Pedro Gomes [d,e], Ana Bettencourt [a,*,1], Isabel A. C. Ribeiro [a,*,2]

[a] Research Institute for Medicines (iMed.ULisboa), Faculty of Pharmacy, Universidade de Lisboa, Avenida Prof. Gama Pinto, 1649-003 Lisboa, Portugal
[b] Faculdade de Ciências e Tecnologia, Universidade Nova de Lisboa, Campus de Caparica, 1829-516 Caparica, Portugal
[c] Centro Interdisciplinar de Estudos Educacionais (CIED), Escola Superior de Educação de Lisboa, Instituto Politécnico de Lisboa, Campus de Benfica do IPL, 1549-003 Lisboa, Portugal
[d] Laboratory for Bone Metabolism and Regeneration – Faculty of Dental Medicine, U. Porto Rua Dr. Manuel Pereira da Silva, 4200-393 Porto, Portugal
[e] LAQV/REQUIMTE, U. Porto, Porto, 4160-007, Portugal
[f] CQE Instituto Superior Técnico, Universidade de Lisboa, Av. Rovisco Pais 1049-001, Lisboa, Portugal
[g] EST Setúbal, CDP2T, Instituto Politécnico de Setúbal, Campus IPS, 2910 Setúbal, Portugal

ARTICLE INFO

Keywords:
Polymer-coating
PDMS
Mesh
Additive manufacturing
Sophorolipids
Surfactin

ABSTRACT

Infections associated with the surfaces of medical devices represent a critical problem due to biofilm formation and the growing resistance towards antibacterial drugs. This is particularly relevant in commonly used invasive devices such as silicone-based ones where a demand for alternative antibiofilm surfaces is increasing. In this work, an antimicrobial chitosan-biosurfactant hydrogel mesh was produced by 3D-printing. The 3D structure was designed to coat polydimethylsiloxane-based medical devices for infection prevention. Additionally, the porous 3D structure allows the incorporation of customized bioactive components. For this purpose, two biosurfactants (surfactin and sophorolipids) were biosynthesized and tested for their antimicrobial activity. In addition, the printing of surfactant-chitosan-based coatings was optimized, and the resulting 3D structures were characterized (i.e., wettability, FTIR-ATR, antimicrobial activity, and biocompatibility). Compared with surfactin, the results showed a better yield and higher antibacterial activity against Gram-positive bacteria for sophorolipids (SLs). Thus, SLs were used to produce chitosan-based 3D-printed coatings. Overall, the SLs-impregnated coatings showed the best antibacterial activity against *Staphylococcus aureus* planktonic bacteria (61 % of growth inhibition) and antibiofilm activity (2 log units reduction) when compared to control. Furthermore, concerning biocompatibility, the coatings were cytocompatible towards human dermal fibroblasts. Finally, the coating presented a mesh suitable to be filled with a model bioactive compound (i.e., hyaluronic acid), paving the way to be used for customized therapeutics.

1. Introduction

Medical devices related-infections are one of the most common complications in the healthcare setting [11]. Common materials such as silicone (polydimethylsiloxane, PDMS) used in the production of the devices may constitute a problem because their abiotic surfaces are prone to microorganism colonization and biofilm development [37]. The formation of biofilms gives specific properties to adhered bacteria that the planktonic ones do not possess. Biofilm bacteria form a highly coordinated and protective 3D structure with specialized zones and specific functions, which allows biofilm bacteria to share nutrients and DNA, helping the survival of the biofilm and increasing antibiotic tolerance [18].

Polymeric coatings have become an increasingly investigated approach to prevent biofilm formation on the surface of medical devices [3]. Different polymers can be used for different biofilm prevention

* Correspondence to: Faculty of Pharmacy, Universidade de Lisboa, Avenida Prof. Gama Pinto, 1649-003 Lisboa, Portugal.
E-mail addresses: asimao@ff.ul.pt (A. Bettencourt), iribeiro@ff.ulisboa.pt (I.A.C. Ribeiro).
[1] ORCID: 0000-0002-8498-5892.
[2] ORCID: 0000-0002-7110-6393.

https://doi.org/10.1016/j.colsurfb.2023.113486
Received 18 April 2023; Received in revised form 10 July 2023; Accepted 30 July 2023
Available online 1 August 2023

strategies. Among those are antifouling polymers conferring repelling properties to surfaces and antimicrobial polymers to produce bactericidal surfaces [15,21,26]. One example of an antibacterial polymer is chitosan (Ch), a linear polysaccharide composed of deacetylated and acetylated units. Its degree of acetylation depends on the ratio of randomly distributed β-(1→4)-linked D-glucosamine and N-acetyl-D--glucosamine monomers [2,6,43]. Its strong positive charge disrupts the bacterial cell membrane, making chitosan an inherently antibacterial polymer that inhibits growth and kills bacteria [26,27].

Furthermore, chitosan can form hydrogels, three-dimensional networks of hydrophilic polymers which can swell, retain large amounts of water, and maintain a well-defined structure [8,22,54]. Additionally, this 3D network makes it a suitable platform for the delivery of bioactive substances to be released over time. [22,29,54]. Many bioactive agents can be incorporated to enhance the inherent antimicrobial activity of chitosan hydrogels, like antibiotics, metals, enzymes, charged organic compounds, antimicrobial peptides, and biosurfactants [10,29]. Among biosurfactants are sophorolipids (SLs) and surfactin (Fig. 1) which are amphipathic molecules containing both hydrophilic and hydrophobic moieties that can also disrupt the bacterial cell membrane and cause cell death [1,44]. These compounds are attracting much interest due to their antimicrobial activity being not prone to the development of resistance and also for presenting antifouling activity related to their surfactant activity [34,37].

With the advent of multiple 3D-printing techniques, the scope of potential applications of polysaccharides combined with other substances is widening, in order to obtain multiple complementary strategies in the same coating [17]. A multifaceted approach could target different stages of the development of biofilms and present a boost effect against bacteria.

Based on the described above, we hypothesized that a 3D-printed antibacterial coating composed of a biosurfactant-chitosan hydrogel with a mesh suitable to be loaded or not with other active agents would reinforce the prevention of infections associated to PDMS-based medical devices. The first part of the work was related to the production and the selection of the biosurfactant (surfactin or sophorolipid) with the highest potential to be included in the coating formulation. In the second part, a 3D-printed coating on a PDMS substrate was developed and characterized. Finally, a chitosan-based hydrogel ink impregnated with the selected biosurfactant to complement the coating with a release-based antibacterial activity was prepared to build the central part of the coating. To evaluate if the produced coating presented a mesh suitable to be loaded with a different hydrogel ink, the hyaluronic acid (HA) hydrogel was used as filler.

2. Materials and methods

2.1. Chemicals and reagents

The carbohydrate polymers used in the presented study were medium molecular weight chitosan with a deacetylation degree of 75–85 % from Sigma-Aldrich (Steinheim, Germany) and hyaluronic acid (30–50k) from Glentham (Corsham, United Kingdom). Other chemicals used were: acetone, methanol, monopotassium phosphate, n-hexane, oleic acid, p-anisaldehyde, acetonitrile (LC-MS grade), potassium nitrate, sodium nitrate, sodium EDTA, and formic acid from Merck (Darmstadt, Germany); ammonium dihydrogen phosphate from BDH Chemicals (UK); barium chloride, chloroform, crystal violet and iron(II) sulfate from Sigma-Aldrich (Steinheim, Germany); di-sodium hydrogen phosphate from VWR chemicals (Leuven, Belgium); ethyl acetate from Honeywell (Seelze, Germany); glacial acetic acid and hydrochloric acid from Scharlau (Barcelona, Spain); glycerol from Vaz Pereira (Lisbon,

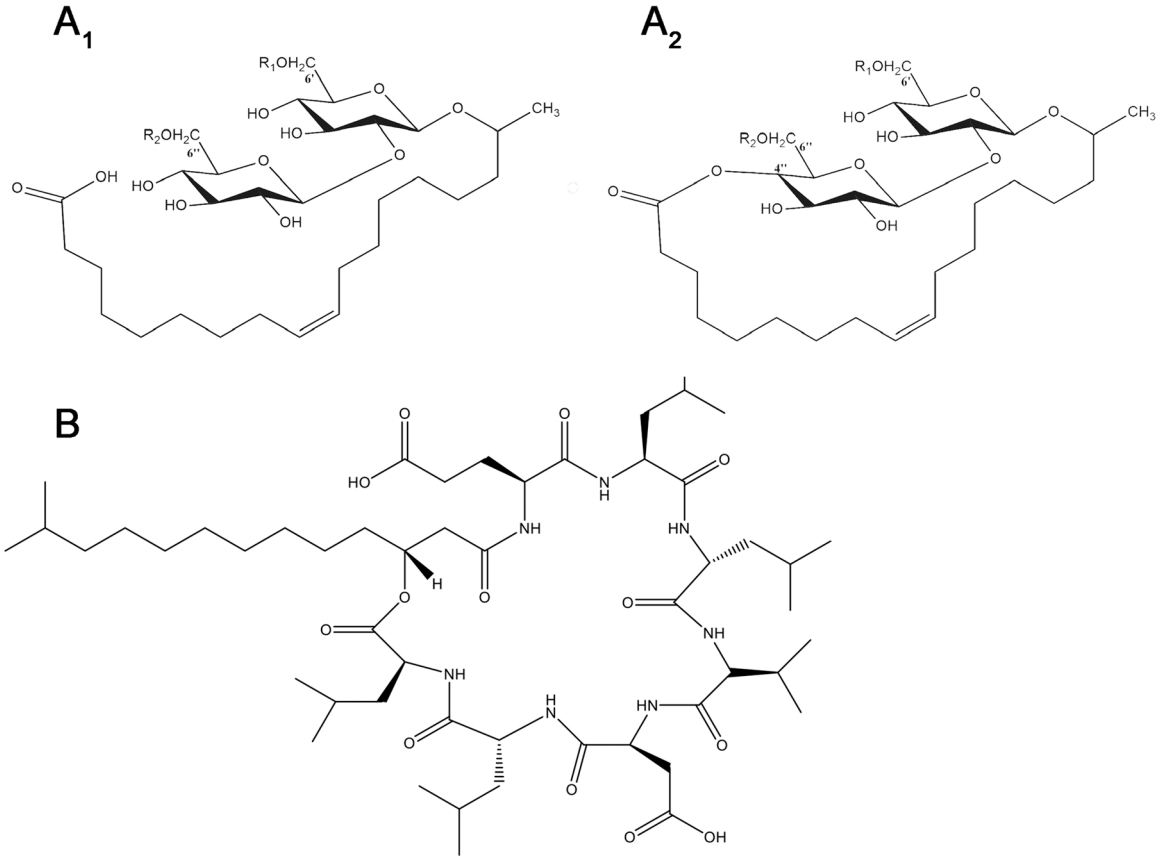

Fig. 1. Sophorolipids in acidic (A_1) and lactonic form (A_2) (R_1 =R_2 =H; R_1 = H and R_2 =$COCH_3$; R_1 = $COCH_3$ and R_2 =H; R_1 =R_2 =$COCH_3$). C14-Surfactin congener (B).

Portugal); calcium chloride, glucose, magnesium sulfate, and sodium chloride from Panreac (Barcelona, Spain); sodium hydroxide from Absolve (Australia). For microbiology assays, the media used were Brain Heart Infusion (BHI) medium, Glucose-Peptone-Yeast Extract (GPY) medium, Mueller-Hinton medium, and Tryptic Soy Agar medium from Biokar (Beauvais, France). Water was purified by a Milli-Q purification system (Millipore).

2.2. Production and extraction of biosurfactants

2.2.1. Microorganisms

Bacillus subtilis ATCC 6633 obtained from the American Type Culture Collection (ATCC) was maintained at 4 °C on Brain Heart Broth (BHI) agar plates with monthly transfers. *Starmerella bombicola* CBS 6009 obtained from the Fungal Biodiversity Centre, CBS (Centraalbureau voor Schimmel) culture was maintained at 4 °C on Glucose-Peptone-Yeast extract (GPY) agar plates, with monthly transfers.

2.2.2. Surfactin production, extraction, and characterization

Pre-cultivation of *B. subtilis* was accomplished in Mineral Salts Medium (MSM) according to Mei et al. [33] with some modifications. The seed medium consisted of glucose (40 g L^{-1}), $NaNO_3$ (20 mM), KNO_3 (30 mM), $Na_2HPO_4{\cdot}12\ H_2O$ (30 mM), $NH_4H_2PO_4$ (50 mM), $CaCl_2$ (0.007 mM), $MgSO_4$ (0.8 mM), sodium EDTA (0.4 mM), and $FeSO_4{\cdot}7\ H_2O$ (0.4 mM). The pre-inoculation of *B. subtilis* was carried out by inoculating 2 colonies in 10 mL of MSM in a 50 mL Erlenmeyer flask which was maintained for 24 h at 30 °C (VWR INCU-Line 150 R incubator) on a orbital shaker (IKA KS 130 basic) at 200 rpm.

The production of surfactin was carried out by transferring the seed medium volume (10 mL) to a 250 mL Erlenmeyer flask containing 100 mL of MSM with the same composition as the seed medium. The production medium was incubated (VWR INCU-Line 150 R incubator) for 72 h or 96 h at 30 °C and 200 rpm on a orbital shaker (IKA KS 130 basic).

At the end of production (72 h and 96 h), the bacterial cells were separated from the remaining broth by centrifugation (4000 rpm, 20 min, 10 °C) in 50 mL falcon tubes. Crude biosurfactant was recovered according to Vaz et al. through acid precipitation [50]. The supernatant was acidified to pH 2.0 using HCl 4 M and left to rest overnight at 4 °C. The resulting precipitate was separated from the remaining broth by centrifugation (4000 rpm, 30 min, 4 °C) in 50 mL tubes. The pellet was then solubilized in 5 mL of MilliQ water, and the pH was adjusted to 7.0 using NaOH 1 M. Surfactin was then purified through dialysis (Float-A-Lyzer G2, MWCO 500–1000D) in MilliQ water for 4 h under gentle stirring (VELP Arex-6 Digital Pro) at room temperature with water replacement every hour.

Finally, the surfactin was lyophilized and stored at − 4 °C [50]. Surfactin mixture characterization was carried out by HPLC-MS using a Waters® Alliance 2695 HPLC system (Waters®, Ireland) coupled to a triple quadrupole mass spectrometer MicroMass Quattromicro® API (Waters®, Ireland). The separation of the compounds was performed using a CORTECS ® C18 column (2.1 ×50 mm, 2.7 μm) at 35 ºC. The mobile phase consisted of water with 0.1 % formic acid as eluent A and acetonitrile as eluent B, at a flow rate of 0.30 mL min^{-1}, with the following gradient program: 0–10 min from 5 % to 50 % B; 10 – 30 min from 50 % to 95 % B; 30–40 min from 95 % to 100 % B; 40–50 min 100 % B, finally returning to the initial conditions for 10 min, as a re-equilibration step. Total run time was 60 min and the injection volume was 10 μL. The mass spectrometry detection was performed using an electrospray ionization (ESI) source operating at 120 ºC, applying a capillary voltage of 3.0 kV. To assess the best MS analytical conditions, a surfactin standard solution was infused through the LC system (without column), and several cone voltages (ranging from 10 −60 V) were assayed. The compounds were ionized in both positive and negative ionization modes and spectra were recorded in the *m/z* 20–2000 Da range. High-purity nitrogen was used as drying and nebulizing gas. MassLynx software (version 4.1) was used to collect data and control analytical conditions.

2.2.3. Sophorolipids production, extraction, and characterization

In this study, SLs production was carried out according to Ribeiro et al. [41,42] as well as SLs extraction. Pre-cultivation of *S. bombicola* in a seed medium for 48 h at 25 °C and 320 rpm was used as inoculum and production took place in GPY medium supplemented with oleic acid 2 % (v/v). Production was maintained for 144 h at 25 °C (VWR INCU-Line 150 R incubator) and 320 rpm (IKA KS 130 basic). After 144 h SLs were extracted by liquid-liquid extraction with ethyl acetate (1:1). The solvent was evaporated in a rotary evaporator (Buchi R-200) at 40 °C and extracts were washed with n-hexane and left to dry overnight. SLs production was confirmed by TLC according to Ribeiro et al. [39,40] and SLs mixture was characterized by UHPLC-MS according to Dardouri et al. [13].

2.3. Antibacterial activity of biosurfactants

The minimum inhibitory concentration of both produced biosurfactants was assessed in Mueller-Hinton (MH) medium by the microdilution assay according to Mendes et al. [34] against *Staphylococcus aureus* ATCC 25923, *Staphylococcus epidermidis* ATCC 28319, and *Escherichia coli* ATCC 25922 obtained from the American Type Culture Collection (ATCC) and *Enterococcus faecalis* NCTC 12697 and *Pseudomonas aeruginosa* NCTC 12903 obtained from the National Collection of Type Culture (NCTC). In a 96-well microtiter plate (MTP) serial dilutions of biosurfactant were performed to reach final assay concentrations ranging from 0.006 to 3 mg mL^{-1}. A levofloxacin solution was also serially diluted to a concentration ranging from 0.03 to 16 μg mL^{-1} for assay validation. Bacteria inoculations had a final concentration of 5×10^5 CFU mL^{-1} and plates were incubated (VWR INCU-Line 150 R incubator) under static conditions for 24 h at 36 °C. Growth inhibition was evaluated by absorbance measurement at 595 nm in Microplate Multimode Detector (Anthos, Zenyth 3100).

2.4. Preparation and optimization of chitosan coatings

2.4.1. Preparation of chitosan gels

Different formulations were tested aiming at selecting the optimal chitosan concentration which granted a good antibacterial activity as well as printability. Chitosan solutions were prepared by dissolving the appropriate amount of medium molecular weight chitosan (w/v) in the appropriate volume of an acetic acid aqueous solution 1 % (v/v) in a glass beaker. The produced gels (i.e. 1 %, 2 %, 2.5 %, and 3 % of chitosan (w/v)) were subsequently magnetically stirred (VELP Arex-6 Digital Pro) for 4 h at 800 rpm at room temperature.

Hydrogels incorporating SLs at 3 mg mL^{-1} were produced with 2.0 % and 2.5 % of chitosan (w/v). Due to the poor water solubility of SLs, glycerol was used to disperse the SLs into the chitosan gel. Thus, SLs were first dissolved in glycerol (Gly) and sonicated (P Selecta Ultrasounds) for 30 min. The dissolved SLs were incorporated into the pre-prepared chitosan gel and stirred (VELP Arex-6 Digital Pro) for another 3 h at 800 rpm at room temperature.

2.4.2. Viscosity evaluation of chitosan gels

The viscosity experiments were carried out on a viscometer (Brookfield Ametek, DVE) at a controlled temperature of 25 °C. To perform the measurement, the gel was transferred into a 15 mL tube and placed in the incubator (VWR INCU-Line 150 R incubator) to reach 25 °C. The viscosity was measured at increasing and then decreasing shear rates. The resulting data was analyzed and viscosity vs shear rate and shear stress vs shear rate graphs were obtained.

2.4.3. Antibiofilm activity of chitosan gels

The antibiofilm assays for chitosan gels were carried out in a 24-well

MTP. Firstly, 0.5 mL of each formulation was poured into the wells of the MTP. The gels were then left to dry at 50 °C for 24 h in an incubator (VWR INCU-Line 150 R incubator). The final assayed volume was 1 mL with a final *S. aureus* concentration of 3×10^6 CFU mL^{-1}. The 24-well MTP was incubated at 36 °C for 24 h under static conditions (VWR INCU-Line 150 R incubator). Wells with and without inoculated medium were used to assess the assay response to biofilm formation in the absence of an inhibitor and the response to culture media (blank), respectively.

Biofilm quantification was achieved by crystal violet assay according to Pontes and co-workers [37]. Wells were washed twice with 1 mL of PBS and fixed with 1 mL of ethanol at 99 % (v/v) for 1 h. Next, samples were stained with 1 mL of 0.1 % (w/v) crystal violet solution for 10 min and then gently washed 3 times with 1 mL of MilliQ water. The remaining crystal violet dye was solubilized in 1 mL of 1 % (v/v) acetic acid ethanolic solution, the resulting solutions were transferred to a 96 wells MTP and absorbance was measured at 595 nm in a Microplate Multimode Detector (Anthos, Zenyth 3100).

In the succeeding data treatment, biofilm inhibition was quantified using the following equation:

$$BI = 100 - \frac{Abs_{sample}}{Abs_{control}} \times 100$$

where BI represents biofilm inhibition (%), Abs_{sample} is the absorbance of the sample, and $Abs_{control}$ is the absorbance of the positive control. The resulting data were expressed as mean and standard deviation (mean ± SD).

2.5. 3D-printing optimization of chitosan coatings

The theoretical conception of the 3D-printed antimicrobial coating can be observed in Fig. 2 A. The main part of the coating consists of a 3D-printed porous structure composed of biosurfactant-impregnated chitosan hydrogel. The 1 × 1 mm pores of the main chitosan coating were filled by a 10 % (w/v) hyaluronic acid aqueous hydrogel (Fig. 2 A).

To assess the parameters which affect the 3D printing of the coatings, multiple assays were carried out with high and low values for each parameter, and a subsequential qualitative evaluation of the printed coatings was performed to reach optimal values. The main evaluated parameters were flow speed, layer height, and number of layers. The tested values for flow speed ranged from 0.15 mm s^{-1} to 1.00 mm s^{-1}. Tested layer heights ranged from 0.25 mm to 0.5 mm and coatings with 2, 3, and 4 layers were tested.

In the printability assays, both the chitosan gel and the hyaluronic acid gel inks were loaded into the adequate syringe and mounted on the 3D-printer (Regemat 3D bioprinter, BIO V1). The hydrogel inks were then used to print square-shaped 10 × 10 mm or 20 × 20 mm coatings with pore sizes of 1 × 1 mm onto medical-grade PDMS. The coatings were photographed before solvent evaporation using a digital microscope (RoHS USB, China) for qualitative evaluation.

Once the optimal values for each parameter were obtained, the resulting coatings were characterized regarding their rheological properties, surface, chemical composition, and antibacterial activity.

2.6. Characterization of chitosan coatings

2.6.1. Viscosity evaluation of chitosan-based hydrogel-ink

The viscosity evaluation of the hydrogel ink was accomplished in the same way as the evaluation of the optimization gels (see. 2.4.2).

2.6.2. Fourier transform infrared spectroscopy attenuated total reflectance (FTIR-ATR)

To evaluate functional groups present on 3D-printed coatings, a Fourier transform infrared spectrophotometer (Thermo Scientific, Class 1 Laser Product Nicolet 6700) with an ATR accessory (split-pea) was used. Spectra ranging from 4000 to 800 cm^{-1} resulting from the average of 32 scans collected with a resolution of 8 cm^{-1} were obtained using OMNIC Software.

2.6.3. Surface wettability

The wettability degree of the different printed coatings was accessed through contact angle measurements that were carried out with the sessile drop method. Ultra-purified (Milli-Q) water drops (2 µL) were deposited on the uncoated and coated surfaces and images were captured with a digital microscope (Rohs Usb Digital Microscope) connected to a computer. Contact angles were evaluated by image analysis using the Image J software. All measurements were performed at room temperature (22 °C) and experiments were evaluated at least in two independent assays with 5 replicates.

2.7. Antibacterial activity of chitosan coatings

The antibacterial assays were carried out in 24 wells MTP. Firstly, 3D-printed coatings covering the surface of 10 × 10 mm medical-grade PDMS squares were fixed to each well. The assays were performed in BHI medium supplemented with glucose (1 % (w/v)) against *S. aureus* at 3×10^6 CFU mL^{-1} in a final assayed volume of 1 mL. Along with the coated samples, plain 10 × 10 mm PDMS squares were also inoculated

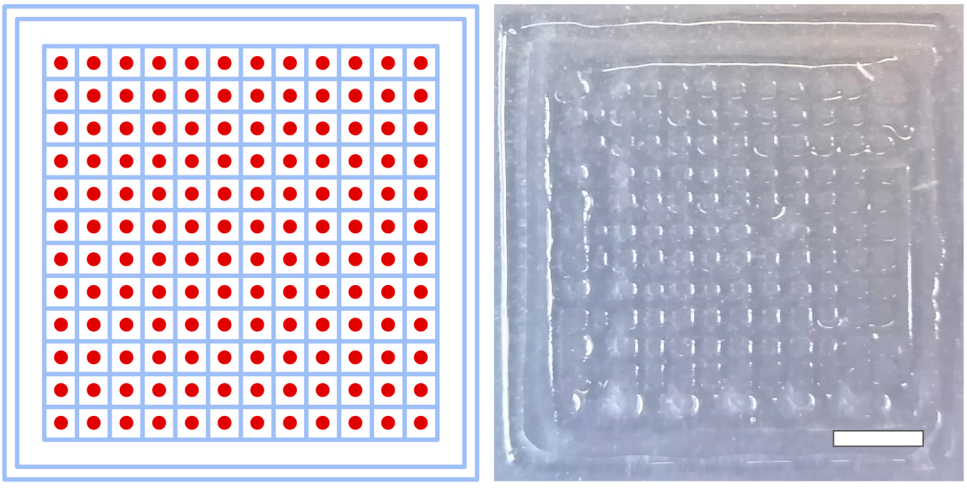

Fig. 2. 3D-Printed coating. Theoretical conceptualization of the 3D printed coating (A). Final 3D-printed coating (Chi 2.5 % + 5 % Gly+SLs) onto a PDMS square: 20 × 20 mm area, 1 × 1 mm pore size, and 0.5 mm height (B). Scale bars: 5 mm.

to determine the antibacterial activity in the absence of an inhibitor. The plates were incubated (VWR INCU-Line 150 R incubator) at 36 °C for 24 h under static conditions. After 24 h, samples were assayed for activity against planktonic and biofilm bacteria after washing each well twice with PBS.

2.7.1. Planktonic bacteria susceptibility

To assess the antibacterial activity of the coatings against planktonic bacteria, the remaining culture media and the two washing solutions (PBS) of each well were collected. The absorbance of the resulting solutions was then measured at 595 nm (Anthos, Zenyth 3100). The obtained absorbance values were converted to CFU mL^{-1} according to the linear regression curve of absorbance vs CFU mL^{-1}.

2.7.2. Biofilm quantification

The antibiofilm activity of the coatings was quantified through the CFU counting method on agar plates according to Mendes et al. [34]. After being twice washed with PBS, the samples were transferred to a 1 mL 0.9 % NaCl solution, sonicated for 4 min, and vortexed for 4 min. The resulting bacterial suspensions were diluted, seeded in TSA plates, and incubated (VWR INCU-Line 150 R incubator) for 24 h at 36 °C. After 24 h, the growing colonies were counted.

2.7.3. Scanning electron microscopy (SEM) of biofilms

Representative samples submitted to a biofilm assay were sequentially fixed with 75 %, 90 % and 100 % (v/v) ethanol solution after being twice washed with PBS. The representative images were acquired on a benchtop SEM, ThermoScientific model Phenom ProX G6, equipped with a CsB6 filament in a mixed 50 % backscattered and 50 % secondary electron mode. To increase the conductivity of the samples a coating of conductive gold film was applied under vacuum in an argon atmosphere (Quorum Technologies, Polaron E5100).

2.8. Biocompatibility of chitosan coatings

Human dermal fibroblasts (HDFs, AG22719), obtained from Coriell Institute for Medical Research, were cultured in α-Minimal Essential Medium (α-MEM), containing 10 % (V/V) of fetal bovine serum (FBS) and 1 % (V/V) of penicillin, streptomycin and amphotericin B (all from Gibco). Cells from the eighth passage were incubated at 37 °C and 5 % CO_2 in the air. After reaching ≈ 70 % confluency, HDFs cells were trypsinized and sub-cultured at 10,000 cells/cm^2. After 24 h, permeable inserts (Transwell 6.5 mm insert, 0.4 μm permeable membrane, Costar) containing chitosan coating samples (2 cm × 2 cm) were placed on the wells, allowing the indirect contact of the materials with the cultures of HDF. Cultures were maintained for 7 days. Adequate controls were established.

2.8.1. Cell viability and metabolic activity

The viability of HDF cultures was evaluated through calcein AM (Biolegend) and Propidium Iodide/RNase (BD Pharmingen) staining, the Live/Dead assay. After 24 h of incubation with the materials, cultures were washed and incubated with the fluorescent solutions for 10–20 min. Images were obtained with a Celena S digital imaging system (Logos Biosystems). For the assessment of the metabolic activity of cultures, a resazurin assay was performed after 1, 3, and 7 days of incubation with materials leachables. Briefly, the culture medium was replaced by a mixture of fresh culture medium with 10 % (V/V) resazurin solution (Sigma-Aldrich) at 0.1 mg mL^{-1}, and HDF cultures were incubated for 3 h at 37 °C. Then, the medium was collected and the fluorescence was measured using a microplate reader (Synergy HT; BioTek - excitation: 530 nm, emission: 590 nm). For the Live/Dead assay, three independent experiments were performed, while five independent experiments were performed for the metabolic activity assay.

2.8.2. Cell morphology

The characterization of the cellular morphology was conducted following F-actin staining using Alexa Fluor 488 (Biolegend) and nucleus counterstaining using Hoechst 33342 (Enzo). After 24 h of incubation with the materials, cells were fixed using paraformaldehyde 3.7 % and permeabilized with Triton-X 0.1 %, before incubation with bovine serum albumin (Sigma-Aldrich). Finally, cells were stained by the fluorescent solutions and observed with a Celena S digital imaging system (Logos Biosystems). Three independent experiments were performed.

3. Results and discussion

3.1. Biosurfactant production and extraction

Surfactin production by *B. subtilis* in MSM was accomplished with yields of 0.847 g L^{-1} and 0.836 g L^{-1} after 72 h and 96 h, respectively. The resulting yields were close to the previously reported in the literature (ranging from 0.23 g L^{-1} to 1.92 g L^{-1}) [23,33,51]. Also, SLs production by *S. bombicola* (6.25 g L^{-1}) after 144 h was consistent with yields reported in previous studies (ranging from 5.95 g L^{-1} to 6.8 g L^{-1}) [7,34]. Different surfactin lipopeptide congeners having chains ranging from C12 to C16, as previously reported by [36] were identified by HPLC-MS, and their corresponding observed protonated molecules are described in Table 1. Sophorolipids identified were mainly lactonic (L) (Table 1) as expected from the production of *S. bombicola* [13]. SLs in their lactonic (L) form have shown to possess a higher antibacterial activity than their acidic (A) forms [55] and may represent an advantage for the studies herein developed.

3.2. Antimicrobial properties of extracted biosurfactants

After the production and extraction of both biosurfactants, the antibacterial activity of surfactin and SLs was tested against planktonic *S. aureus*, *S. epidermidis*, *E. coli*, *E. faecalis,* and *P. aeruginosa* by assessing the minimum inhibitory concentration (MIC) (Table 2).

Both biosurfactants showed higher antibacterial activity against Gram-positive bacteria which is in accordance with previous observations [46]. Surfactin and SLs were able to inhibit the growth of *S. aureus*, *E. faecalis*, and *S. epidermidis* with concentrations ranging from 0.023 mg mL^{-1} to 0.750 mg mL^{-1}. However, no biosurfactant was able to inhibit *P. aeruginosa* or *E. coli* under the tested conditions. Furthermore, the antibacterial activity against planktonic bacteria of SLs consistently outperformed surfactin activity. MIC assays were conducted to choose the most active biosurfactant to be incorporated in the coating formulation. Thus, SLs were chosen over surfactin to proceed with further studies.

Table 1
Identified compounds by HPLC-MS present in biosurfactant mixtures.

Surfactins	MW	$[M + H]^+$	Sophorolipids (SLs)	MW	$[M + Na]^+$
Surfactin C12	994	995	A–C18:1 monoacetylated	664	687
Surfactin C13	1008	1009	A-C18:1 diacetylated	706	729
Surfactin C14	1022	1023	L–C18:1 monoacetylated	646	689
Surfactin C15	1036	1037	L-C18:2 diacetylated	686	709
Surfactin C16	1050	1051	L-C16:0 diacetylated	662	685
			L-C18:1 diacetylated	688	711
			L-C18:0 diacetylated	690	713

Table 2
Minimum inhibitory concentration expressed in mg mL^{-1} for surfactin and SLs against Gram-positive and Gram-negative bacteria.

Bacteria	Surfactin (mg mL^{-1})	SLs (mg mL^{-1})
E. coli ATCC 25922	>3.00	>3.00
E. faecalis NCTC 12697	0.188	0.047
P. aeruginosa NCTC 12903	>3.00	>3.00
S. aureus ATCC 25923	0.047	0.023
S. epidermidis ATCC 28319	0.750	0.047

3.3. Coatings production

3.3.1. Optimization of Chitosan coatings

Following the selection of the active agent to be incorporated in the final hydrogel formulation, a viscosity assessment was carried out to guarantee the printability of the hydrogel. Thus, to determine the appropriate concentration of chitosan (Ch) to be used in the ink formulation, the viscosity of the gels with different Ch percentages (1 %, 2 %, and 2.5 %) was studied. All the gels presented a shear thinning behavior characterized by the decrease of the viscosity as the shear rate increases (SM 1). Moreover, the results showed a time-dependent decrease in the apparent viscosity, meaning that the Ch2 % and Ch2.5 % gels were thixotropic. It was also possible to observe a viscosity increase along with the increase in chitosan concentration. The rheological results were consistent with previous studies which also reported a non-Newtonian shear-thinning behavior [31]. The viscosity of the hydrogel ink is a very relevant factor due to its significant effects on printability. On the one hand, it should be low enough to allow an easy ink extrusion through the syringe nozzle. On the other hand, it should be high enough to allow adhesion, with no collapsing, and create a stable structure [24,32].

Among the tested gels, the Ch3 % was determined to be too viscous to be used as a printable gel. The high viscosity of this gel made it very hard to extrude through the nozzle of the syringe, resulting in a very granular coating with non-fused layers. On the contrary, the Ch1 % presented a low viscosity for extrudable ink use. The low viscosity of the gel would make the layers of the coating collapse onto themselves resulting in a poorly defined 3D structure. Hence, the gels chosen as potential inks and submitted to further tests were Ch2 % and Ch2.5 %.

The next step in the optimization of the ink formulation was assessing the antibiofilm activity of the selected gels. Here, the biofilm inhibition of the chitosan gels (Ch2 % and Ch2.5 %) with and without SLs (3 mg mL^{-1}) was tested. The results (SM2) confirmed the antibiofilm activity of chitosan, which was to be expected due to its inherent antibacterial activity which was corroborated in several previous studies. [16,26,27]. Additionally, SLs had already shown their ability to inhibit the formation of biofilms in previous studies [34,49]. However, it was essential to understand if the activity of SLs was not hindered by their incorporation into the chitosan gels. The highest antibacterial activity in the assays was obtained in the gels incorporating SLs (SM2). Thus, when comparing both chitosan concentrations, it was determined a slightly better antibiofilm activity for the Ch2.5 % added of SLs, therefore, this formulation was selected to be tested in the subsequent printing studies.

After the hydrogel-ink formulation selection, it was assessed which printing configurations generated the coatings on the silicon surface closest to the projected model. The parameters which most significantly affected the quality of the coating were flow speed, layer height, and number of layers. Regarding the flow speed parameter, the results (SM 3 A) showed that higher flow speed values resulted in an excessive extrusion of the ink which produced coatings lacking the pores intended to accommodate the hyaluronic acid hydrogel. In contrast, lower flow speed values originated incomplete structures due to a low amount of extruded ink (SM 3B). Regarding the parameters layer height and the number of layers in SM 3 C it can be observed that shorter layers and, therefore, a higher number of layers, originated 3D-coatings with a poorly defined structure due to the collapse of the extruded layers. However, in SM 3D, coatings with a lower number of higher layers resulted in a better-defined structure.

Hence, the final parameters chosen for the printing of the chitosan coating were a layer height of 0.25 mm, a layer number of 2, and a flow speed of 0.6 mm s^{-1} (Fig. 2). Furthermore, the final 3D structures were printed in a 20 × 20 mm area of a PDMS surface for more efficient production.

Finally, after the 3D-printed coating optimization, characterization regarding the rheological properties of the ink, surface properties, and antibacterial activity was carried out. Comparing the final ink in Fig. 3 with the previously tested chitosan gels (SM 2), it was possible to assess that the supplementation with glycerol and SLs did not affect the viscosity of the mixtures in any major way. Moreover, just like the pristine chitosan gels, the final selected ink also exhibited a shear thinning behavior and thixotropy (Fig. 3).

The final structure of the printed coating was intended as a multifaceted approach to prevent bacterial infection. The main coating component would be chitosan-based to grant a contact-killing antibacterial activity. The combination of chitosan with SLs would allow a complementary release-based antibacterial activity. Furthermore, the pores of the coating were filled with hyaluronic acid hydrogel that has been cited in other works for its antifouling activity [43]. Thus, the complexity of this 3D structure was able to be produced through 3D-printing technology and further characterized and tested for biological activity.

3.4. Characterization of chitosan-based coatings

The FTIR-ATR spectra of the coating samples are shown in Fig. 4A. For chitosan, characteristic absorption bands were observed at 3355 cm^{-1} (hydroxyl groups), 2886 cm^{-1} (C-H bonds), 1608 cm^{-1} (C-N bonds), and 1652 cm^{-1} (carbonyl groups) [19,28,48]. Moreover, characteristic bands for SLs could be observed at 3355 cm^{-1}, and 2886 and 2937 cm^{-1} for hydroxyl groups and C-H bonds, respectively [6,37]. Hyaluronic acid exhibited bands at 3355 cm^{-1} (hydroxyl groups), 2886 cm^{-1} (C-H bonds), 1417 cm^{-1} (COO stretching), 1031 cm^{-1} (C-O-H bending vibration), and 1608 cm^{-1} (C-N bonds) [53]. Additionally, it can be observed that there were no additional bands in the spectra of the chitosan coatings with SLs and HA, indicating that the formation of Ch+SLs+HA was a simple physical mixture.

The wettability degree of a surface can be assessed through its water contact angle measurement. Higher water contact angles correspond to lower wettability degrees whilst lower angles correspond to higher wettability degrees [37].

Fig. 4B shows the measured water contact angles on PDMS and different 3D-printed coatings. It is possible to observe that all the produced coatings reduced the water contact angle comparatively with PDMS. The lowest reduction corresponds to the Ch coating and the highest observed reduction corresponds to the SLs-supplemented formulations. The wettability degree of a surface has previously been shown to be linked with its ability to restrain bacterial colonization [30,35]. A lower wettability degree indicates a hydrophobic surface which aids the attachment of hydrophobic bacteria like *S. aureus* [38,53]. On the other hand, a more hydrophilic surface, presenting a lower water contact angle hinders this attachment [30,38]. Thus, a coating that enhances the wettability degree of a surface leads to an improved ability to prevent *S. aureus* adhesion.

3.5. Antibacterial activity of chitosan-based coatings

Antimicrobial susceptibility of planktonic bacteria when in contact with the coating was evaluated by measuring the absorbance of the remaining culture medium (Fig. 5A). The number of planktonic cells associated with control samples (i.e. in the absence of coating) was

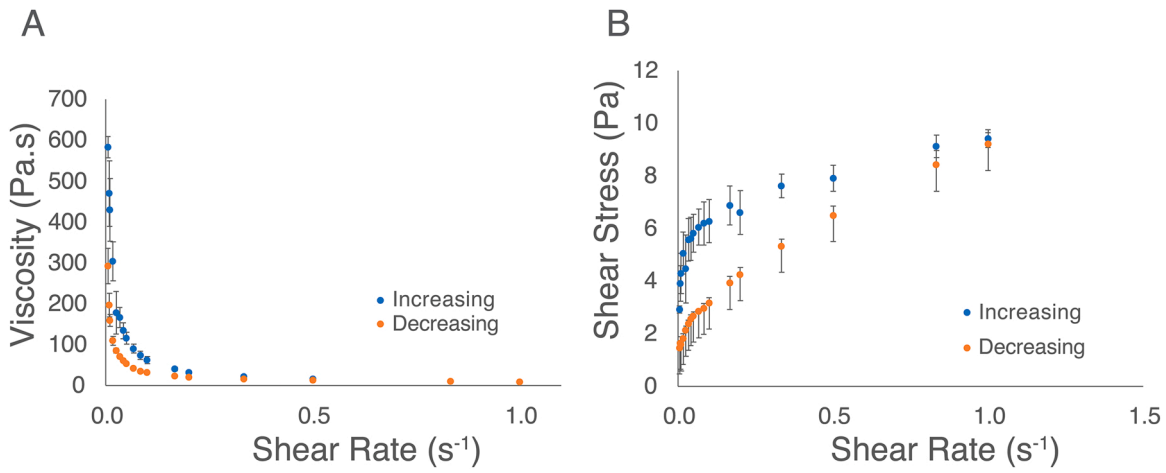

Fig. 3. Viscosity evaluation of SLs (3 mg mL^{-1}) impregnated chitosan gels showing a non-Newtonian shear-thinning and thixotropic behavior. Viscosity as a function of the shear rate of chitosan-based optimized ink with ascending and descending shear rate values (A). Shear stress as a function of the shear rate of chitosan-based optimized ink with ascending and descending shear rate values (B).

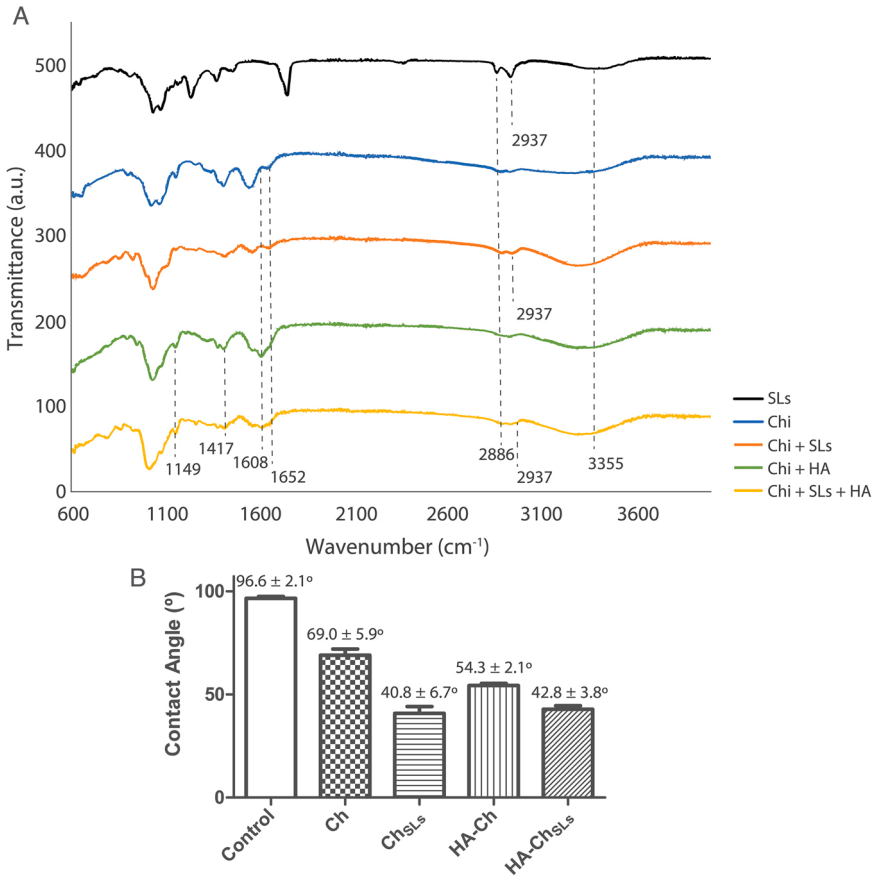

Fig. 4. FTIR-ATR spectra for SLs and different chitosan-based coatings showing characteristic bands of their functional groups (A). Water contact angle of different 3D-printed chitosan-based coatings and PDMS. All the contact angle values are expressed as an average replicate experiments and respective standard deviations (B). Contact angle measurements were performed on PDMS (Control), Ch coating, Ch_{SLs} coating, HA-Ch coating, and HA-Ch_{SLs} coating.

$\backsimeq 5.4 \times 10^8$ CFU mL^{-1}. Regarding the coated samples, Ch coatings showed some inhibition of planktonic cells due to the inherent antibacterial properties of chitosan. Moreover, coatings containing SLs (Ch_{SLs}) showed the highest growth inhibition (61 %). On the other hand, the HA-Ch coatings showed the lowest antibacterial activity against planktonic bacteria among all other coatings.

The antibiofilm activity of the coatings against *S. aureus* was evaluated by biofilm CFU counts (Fig. 5B). Among all coatings the best antibiofilm activity was observed for the Ch_{SLs} followed by the Ch coating, reaching an almost 2-log inhibition and 1.5-log inhibition of bacterial growth, respectively.

Although the filling of the Ch_{SL} mesh with hyaluronic acid led to some activity against planktonic *S. aureus*, when evaluating biofilm prevention, the result was not so promising. This may be related to the fact that the antifouling effect of hyaluronic acid is concentration-dependent [20] suggesting that the tested amount was not high

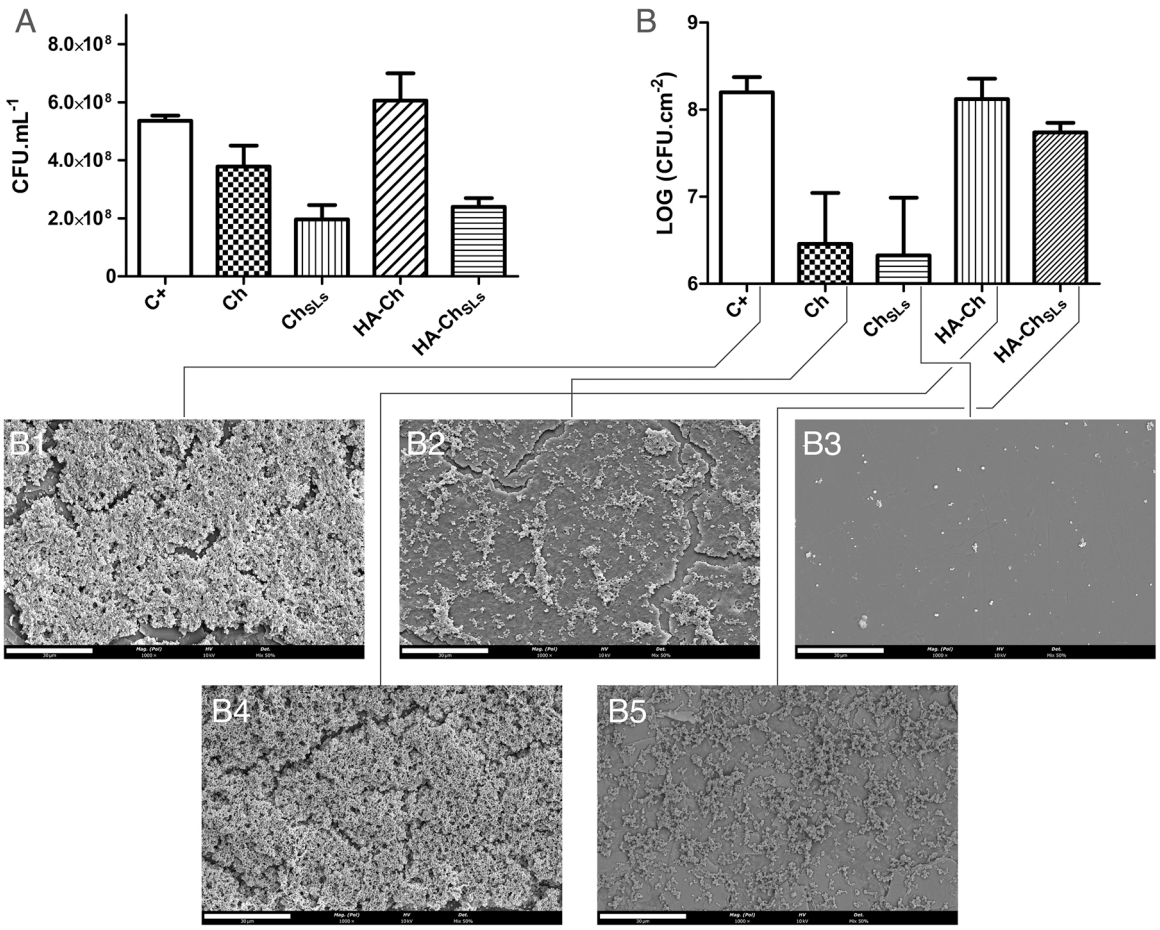

Fig. 5. Inhibition of planktonic (A) and sessile (B) *S. aureus* for PDMS (C+), Ch coating, Ch_{SLs} coating, HA-Ch coating, and HA-Ch_{SLs} coating. SEM images of *S. aureus* biofilm on representative PDMS segments: PDMS (B_1); Ch coating (B_2); Ch_{SLs} coating (B_3); HA-Ch coating (B_4); HA-Ch_{SLs} coating (B_5). Scale bars: 30 μm.

enough to have a positive antibiofilm effect and covered in part the chitosan film blocking its activity.

To further confirm the previous results, SEM qualitative analysis of representative samples allowed the visualization of formed biofilm on each sample (Fig. 5 B_1-B_5). In general, the SEM results were consistent with the CFU counting results. Coatings with the least attachment of bacteria were the ones containing SLs and no HA in their composition (Ch_{SLs}) which is in accordance with the antibiofilm assays. Thus, the coating with the best antibiofilm activity is based on the inherent antibacterial properties of chitosan, as it is generally corroborated by previous studies [4,16,26,27], and a release-based approach of sophorolipids which is also following previous reports [34].

3.6. Biocompatibility of chitosan-based coatings

The cytocompatibility of chitosan coatings was evaluated using human dermal fibroblasts due to their structural and organizational relevance to connective tissues and immunomodulatory activity [52]. HDF cultures presented high viability at day 1 of culture, evaluated by the resazurin and live/dead assays, and a continuously increased metabolic activity until day 7 when grown in indirect contact with PDMS samples (Fig. 6-A and B). Regarding cellular morphology, cultures were found to be well spread through the bottom of the culture plate, with an elongated and stretched shape and cytoplasmic parallel stress fibers organization. The presence of cytoplasmic extensions and filopodia evidenced numerous intercellular contacts, demonstrating adequate cellular functionality (Fig. 6-C).

In the presence of the coated materials, equivalent cellular behavior was observed, confirming the cytocompatibility of the distinct chitosan-based coatings (Fig. 6). Samples presented a similar metabolic activity pattern throughout the culture period and analogous viability, assessed through the resazurin and live/dead cell assays (Fig. 6-A and B). Among experimental groups, significant differences were only noted in the metabolic activity at day 3, which was higher in HDFs cultured with HA-containing materials in comparison to PDMS and Ch_{SLs} samples. This finding might be due to the antioxidant capabilities of HA, which binds to and inactivates ROS [9], favoring cell viability and, therefore, may increase the metabolic activity of cultures. In addition, HDF cells express CD44 receptors; which interact directly with HA, possibly influencing cell adhesion, migration, and proliferation via activation of the ERK/-MAPK signaling cascade [25]. Furthermore, HA-CD44 interactions may further signal to increase in Ca^{2+} influx, essential for cell cycle progression and cell proliferation, as previously demonstrated for diverse cell types [25]. Cell morphology was indistinguishable between the control and experimental groups (Fig. 6-C).

In a sense, the obtained results are expected, since all compounds (PDMS, chitosan, HA, and sophorolipids) have proven biocompatibility, inducing an adequate cellular response, as reported by several studies [6,12]. Chitosan is known for its low toxicity profile, being employed in diverse platforms (e.g., catheters, hydrogels, and particles) targeting a wide range of clinical applications aiming the direct contact with living tissues - from epithelial wounds to the management of neurological diseases [45].

Moreover, the addition of HA to chitosan can further enhance its hydrophilicity, favoring the overall cytocompatibility of the material, as verified by Bazmandeh et al. and Silvestro et al. [5,47]. Regarding sophorolipids, although previous studies reported possible dose-dependent cytotoxicity [14,34], no significant adverse effects were

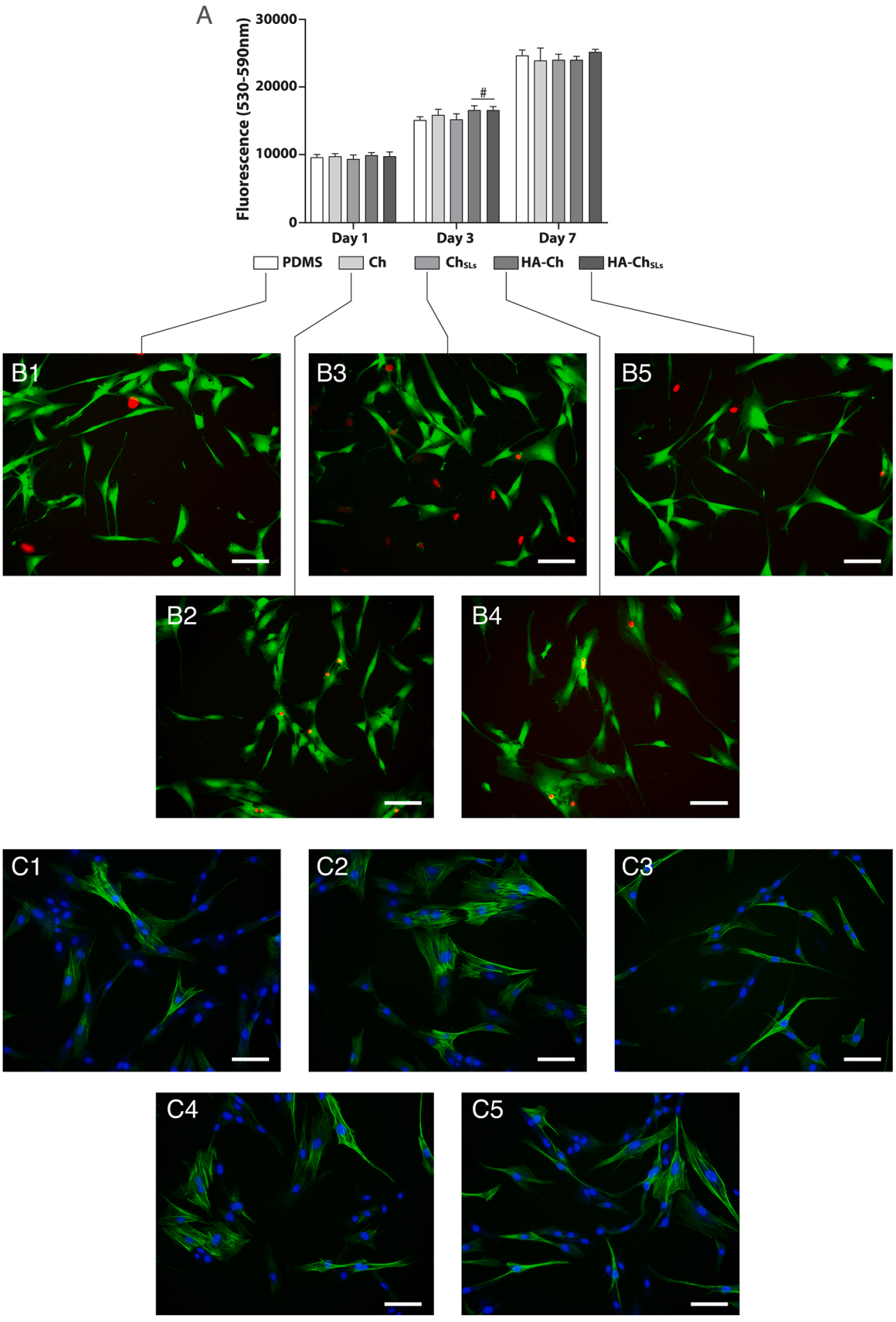

Fig. 6. Cytocompatibility assessment of the chitosan coatings by HDFs cultures grown in indirect contact. (A) Representative images of the live/dead assay (cell viability) at day 1, where live cells display green fluorescence and dead cells show red fluorescence. (B) Resazurin assay (metabolic activity) over seven days of culture. # Significantly different from PDMS and ChSLs groups ($p < 0.05$). (C) Representative fluorescence images of cell morphology on day 1. The actin cytoskeleton was stained in green, and nuclei were counterstained in blue. PDMS (C1); Ch (C2); ChSLs (C3); HA-Ch (C4); HA-ChSLs (C5). Scale bars: 100 μm.

observed in the present study, expectedly associated with the use of subtoxic amounts. Regarding sophorolipids, despite previous studies reporting possible dose-dependent cytotoxicity [14,34], no significant adverse effects were observed in the present study, expectedly associated with the use of subtoxic amounts.

4. Conclusions

Mesh-based coatings of SLs-chitosan were successfully printed on PDMS substrates. Optimization of the printing conditions and hydrogel formulation were needed and a suitable hydrogel ink was achieved with chitosan at 2.5 % (w/v). The antimicrobial activity of the chitosan hydrogel ink was reinforced with the addition of sophorolipids (3 mg mL^{-1}) produced by *S. bombicola*. Attained Ch_{SLs} hydrogel showed to be suitable to produce a mesh-based coating intended/ or not to be loaded with additional components to gather extra properties of the coating (e.g., customized properties). The produced 3D-printed Ch_{SLs} hydrogel coating showed a reduction of the contact angle and a decrease in the number of planktonic and biofilm *S. aureus*. A biofilm formation reduction (almost 2 log units) was observed for the Ch_{SLs} coatings. Regarding biocompatibility, all tested coatings showed adequate cytocompatibility and no adverse effects against human dermal fibroblasts.

Overall, the used hydrogel inks showed appropriate printability. The developed 3D-printed coatings demonstrated a solid capability to be used as antibacterial coatings for PDMS-based medical devices although further studies are necessary, namely to demonstrate that the hydrogel is active for long-term periods.

CRediT authorship contribution statement

Francisco Narciso: Methodology, Formal analysis, Investigation, Writing – original draft. **Sara Cardoso:** Methodology, Formal analysis, Investigation. **Nuno Monge:** Visualization, Project administration. **Madalena Lourenço:** Formal analysis. **Victor Martin:** Investigation, Methodology. **Noélia Duarte:** Methodology. **Catarina Santos:** Formal analysis. **Pedro Gomes:** Supervision, Writing – review & editing. **Ana Bettencourt:** Writing – review & editing. **Isabel A.C. Ribeiro:** Conceptualization Validation, Supervision, Resources, Writing—review and editing.

Declaration of Competing Interest

The authors declare that they have no known competing financial interests or personal relationships that could have appeared to influence the work reported in this paper.

Data availability

Data will be made available on request.

Acknowledgements

The authors would like to thank the Portuguese government, Fundação para a Ciência e Tecnologia (FCT), for the financial support through national funds PTDC/BTM-SAL/29335/2017, under iMed. ULisboa UIDB/04138/2020 and UIDP/04138/2020 and under IPL IPL/2022/3DWounDres_ESELx. FCT is also acknowledged for the research initiation Grant BII/2/FF/2022. The authors acknowledge the financial support from FCT and Portugal 2020 to the Portuguese Mass Spectrometry Network (Rede Nacional de Espectrometria de Massa – RNEM; LISBOA-01-0145-FEDER-402-022125). The authors also acknowledge Andreia Bento da Silva (FFUL) for the assistance with the HPLC-MS equipment and Isabel Nogueira (IST Microlab) for the assistance with SEM imaging.

Appendix A. Supporting information

Supplementary data associated with this article can be found in the online version at doi:10.1016/j.colsurfb.2023.113486.

References

[1] V. Abbot, D. Paliwal, A. Sharma, P. Sharma, A review on the physicochemical and biological applications of biosurfactants in biotechnology and pharmaceuticals, Heliyon 8 (8) (2022), e10149, https://doi.org/10.1016/j.heliyon.2022.e10149.
[2] A. Aguanell, M.L. del Pozo, C. Pérez-Martín, G. Pontes, A. Bastida, A. Fernández-Mayoralas, E. García-Junceda, J. Revuelta, Chitosan sulfate-lysozyme hybrid hydrogels as platforms with fine-tuned degradability and sustained inherent antibiotic and antioxidant activities, Carbohydr. Polym. 291 (2022), 119611, https://doi.org/10.1016/j.carbpol.2022.119611.
[3] U. Ajdnik, M. Finšgar, L. Fras Zemljič, Characterization of chitosan-lysine surfactant bioactive coating on silicone substrate, Carbohydr. Polym. 232 (2020), 115817, https://doi.org/10.1016/j.carbpol.2019.115817.
[4] I. Aranaz, A.R. Alcántara, M.C. Civera, C. Arias, B. Elorza, A. Heras Caballero, N. Acosta, Chitosan: an overview of its properties and applications, Polymers 13 (19) (2021) 3256, https://doi.org/10.3390/polym13193256.
[5] A.Z. Bazmandeh, E. Mirzaei, Y. Ghasemi, M.A.J. Kouhbanani, Hyaluronic acid coated electrospun chitosan-based nanofibers prepared by simultaneous stabilizing and coating, Int. J. Biol. Macromol. 138 (2019) 403–411, https://doi.org/10.1016/j.ijbiomac.2019.07.107.
[6] A.F. Bettencourt, C. Tomé, T. Oliveira, V. Martin, C. Santos, L. Gonçalves, M. H. Fernandes, P.S. Gomes, I.A.C. Ribeiro, Exploring the potential of chitosan-based particles as delivery-carriers for promising antimicrobial glycolipid biosurfactants, Carbohydr. Polym. 254 (2021), 117433, https://doi.org/10.1016/j.carbpol.2020.117433.
[7] F.A. Bezza, E.M.N. Chirwa, Production and applications of lipopeptide biosurfactant for bioremediation and oil recovery by Bacillus subtilis CN2, Biochem. Eng. J. 101 (2015) 168–178, https://doi.org/10.1016/j.bej.2015.05.007.
[8] N. Bhattarai, J. Gunn, M. Zhang, Chitosan-based hydrogels for controlled, localized drug delivery, Adv. Drug Deliv. Rev. 62 (1) (2010) 83–99, https://doi.org/10.1016/j.addr.2009.07.019.
[9] N. Cirillo, A. Vicidomini, M. McCullough, A. Gambardella, Y. Hassona, S.S. Prime, G. Colella, A hyaluronic acid-based compound inhibits fibroblast senescence induced by oxidative stress in vitro and prevents oral mucositis in vivo, J. Cell. Physiol. 230 (7) (2015) 1421–1429, https://doi.org/10.1002/jcp.24908.
[10] M. Cloutier, D. Mantovani, F. Rosei, Antibacterial coatings: challenges, perspectives, and opportunities, Trends Biotechnol. 33 (11) (2015) 637–652, https://doi.org/10.1016/j.tibtech.2015.09.002.
[11] N.C.T. Dadi, B. Radochová, J. Vargová, H. Bujdáková, Impact of healthcare-associated infections connected to medical devices—an update, Microorganisms 9 (11) (2021) 2332, https://doi.org/10.3390/microorganisms9112332.
[12] M. Dardouri, A. Bettencourt, V. Martin, F.A. Carvalho, B. Colaço, A. Gama, M. Ramstedt, N.C. Santos, M.H. Fernandes, P.S. Gomes, I.A.C. Ribeiro, Assuring the biofunctionalization of silicone covalently bonded to Rhamnolipids: antibiofilm activity and biocompatibility, Pharmaceutics 14 (9) (2022) 1836, https://doi.org/10.3390/pharmaceutics14091836.
[13] M. Dardouri, R.M. Mendes, J. Frenzel, J. Costa, I.A.C. Ribeiro, Seeking faster, alternative methods for glycolipid biosurfactant characterization and purification, Anal. Bioanal. Chem. 413 (16) (2021) 4311–4320, https://doi.org/10.1007/s00216-021-03387-4.
[14] A. Daverey, K. Dutta, S. Joshi, A. Daverey, Sophorolipid: a glycolipid biosurfactant as a potential therapeutic agent against COVID-19, Bioengineered 12 (2) (2021) 9550–9560, https://doi.org/10.1080/21655979.2021.1997261.
[15] Y. Delaviz, J.P. Santerre, D.G. Cvitkovitch, Infection resistant biomaterials. in: Biomaterials and Medical Device - Associated Infections, Elsevier, 2015, pp. 223–254, https://doi.org/10.1533/9780857097224.2.223.
[16] F. Devlieghere, A. Vermeulen, J. Debevere, Chitosan: antimicrobial activity, interactions with food components and applicability as a coating on fruit and vegetables, Food Microbiol. 21 (6) (2004) 703–714, https://doi.org/10.1016/j.fm.2004.02.008.
[17] L. Diaz-Gomez, I. Gonzalez-Prada, R. Millan, A. Da Silva-Candal, A. Bugallo-Casal, F. Campos, A. Concheiro, C. Alvarez-Lorenzo, 3D printed carboxymethyl cellulose scaffolds for autologous growth factors delivery in wound healing, Carbohydr. Polym. 278 (2022), 118924, https://doi.org/10.1016/j.carbpol.2021.118924.
[18] G. Donelli, Vascular catheter-related infection and sepsis, Surg. Infect. 7 (supplement 2) (2006) s-25–s-27, https://doi.org/10.1089/sur.2006.7.s2-25.
[19] A. Drabczyk, S. Kudłacik-Kramarczyk, M. Głąb, M. Kędzierska, A. Jaromin, D. Mierzwiński, B. Tyliszczak, Physicochemical investigations of chitosan-based hydrogels containing aloe vera designed for biomedical use, Materials 13 (14) (2020) 3073, https://doi.org/10.3390/ma13143073.
[20] L. Drago, L. Cappelletti, E. De Vecchi, L. Pignataro, S. Torretta, R. Mattina, Antiadhesive and antibiofilm activity of hyaluronic acid against bacteria responsible for respiratory tract infections, APMIS 122 (10) (2014) 1013–1019, https://doi.org/10.1111/apm.12254.
[21] I. Francolini, C. Vuotto, A. Piozzi, G. Donelli, Antifouling and antimicrobial biomaterials: an overview, APMIS 125 (4) (2017) 392–417, https://doi.org/10.1111/apm.12675.

[22] M. Fu, Y. Liang, X. Lv, C. Li, Y.Y. Yang, P. Yuan, X. Ding, Recent advances in hydrogel-based anti-infective coatings, J. Mater. Sci. Technol. 85 (2021) 169–183, https://doi.org/10.1016/j.jmst.2020.12.070.
[23] N.G. Ganesan, V. Rangarajan, A kinetics study on surfactin production from Bacillus subtilis MTCC 2415 for application in green cosmetics, Biocatal. Agric. Biotechnol. 33 (2021), 102001, https://doi.org/10.1016/j.bcab.2021.102001.
[24] F.C. Godoi, S. Prakash, B.R. Bhandari, 3d printing technologies applied for food design: status and prospects, J. Food Eng. 179 (2016) 44–54, https://doi.org/10.1016/j.jfoodeng.2016.01.025.
[25] J. Hwang, K.L. Kiick, M.O. Sullivan, Modified hyaluronic acid-collagen matrices trigger efficient gene transfer and prohealing behavior in fibroblasts for improved wound repair, Acta Biomater. 150 (2022) 138–153, https://doi.org/10.1016/j.actbio.2022.07.039.
[26] A. Jain, L.S. Duvvuri, S. Farah, N. Beyth, A.J. Domb, W. Khan, Antimicrobial polymers, Adv. Healthc. Mater. 3 (12) (2014) 1969–1985, https://doi.org/10.1002/adhm.201400418.
[27] N.F. Kamaruzzaman, L.P. Tan, R.H. Hamdan, S.S. Choong, W.K. Wong, A.J. Gibson, A. Chivu, M. de F. Pina, Antimicrobial polymers: the potential replacement of existing antibiotics? Int. J. Mol. Sci. 20 (11) (2019) 2747, https://doi.org/10.3390/ijms20112747.
[28] I.Y. Kim, S.J. Kim, M.-S. Shin, Y.M. Lee, D.-I. Shin, S.I. Kim, pH- and thermal characteristics of graft hydrogels based on chitosan and poly(dimethylsiloxane, J. Appl. Polym. Sci. 85 (13) (2002) 2661–2666, https://doi.org/10.1002/app.10626.
[29] D.M. Kirchmajer, R. Gorkin III, M. in het Panhuis, An overview of the suitability of hydrogel-forming polymers for extrusion-based 3D-printing, J. Mater. Chem. B 3 (20) (2015) 4105–4117, https://doi.org/10.1039/C5TB00393H.
[30] M. Li, X. Liu, N. Liu, Z. Guo, P.K. Singh, S. Fu, Effect of surface wettability on the antibacterial activity of nanocellulose-based material with quaternary ammonium groups, Colloids Surf. A Physicochem. Eng. Asp. 554 (2018) 122–128, https://doi.org/10.1016/j.colsurfa.2018.06.031.
[31] I.M. Lipatova, A.A. Yusova, N.V. Losev, E.A. Indeikin, Gelation in solutions of low deacetylated chitosan initiated by high shear stresses, Int. J. Biol. Macromol. 139 (2019) 550–557, https://doi.org/10.1016/j.ijbiomac.2019.07.164.
[32] Z. Liu, M. Zhang, B. Bhandari, C. Yang, Impact of rheological properties of mashed potatoes on 3D printing, J. Food Eng. 220 (2018) 76–82, https://doi.org/10.1016/j.jfoodeng.2017.04.017.
[33] Y. Mei, Z. Yang, Z. Kang, F. Yu, X. Long, Enhanced surfactin fermentation via advanced repeated fed-batch fermentation with increased cell density stimulated by EDTA–Fe (II), Food Bioprod. Process. 127 (2021) 288–294, https://doi.org/10.1016/j.fbp.2021.03.012.
[34] R.M. Mendes, A.P. Francisco, F.A. Carvalho, M. Dardouri, B. Costa, A. F. Bettencourt, J. Costa, L. Gonçalves, F. Costa, I.A.C. Ribeiro, Fighting S. aureus catheter-related infections with sophorolipids: electing an antiadhesive strategy or a release one? Colloids Surf. B Biointerfaces 208 (2021), 112057 https://doi.org/10.1016/j.colsurfb.2021.112057.
[35] R. Paneru, S.H. Ki, P. Lamichhane, L.N. Nguyen, B.C. Adhikari, I.J. Jeong, S. Mumtaz, J. Choi, J.S. Kwon, E.H. Choi, Enhancement of antibacterial and wettability performances of polyvinyl alcohol/chitosan film using non-thermal atmospheric pressure plasma, Appl. Surf. Sci. 532 (2020), 147339, https://doi.org/10.1016/j.apsusc.2020.147339.
[36] Y. Pecci, F. Rivardo, M.G. Martinotti, G. Allegrone, LC/ESI-MS/MS characterisation of lipopeptide biosurfactants produced by the Bacillus licheniformis V9T14 strain, J. Mass Spectrom. 45 (7) (2010) 772–778, https://doi.org/10.1002/jms.1767.
[37] C. Pontes, M. Alves, C. Santos, M.H. Ribeiro, L. Gonçalves, A.F. Bettencourt, I.A. C. Ribeiro, Can Sophorolipids prevent biofilm formation on silicone catheter tubes, Int. J. Pharm. 513 (1–2) (2016) 697–708, https://doi.org/10.1016/j.ijpharm.2016.09.074.
[38] F. Reifsteck, S. Wee, B.J. Wilkinson, Hydrophobicity–hydrophilicity of staphylococci, J. Med. Microbiol. 24 (1) (1987) 65–73, https://doi.org/10.1099/00222615-24-1-65.
[39] I.A. Ribeiro, M.R. Bronze, M.F. Castro, M.H.L. Ribeiro, Optimization and correlation of HPLC-ELSD and HPLC–MS/MS methods for identification and characterization of sophorolipids, J. Chromatogr. B 899 (2012) 72–80, https://doi.org/10.1016/j.jchromb.2012.04.037.
[40] I.A. Ribeiro, M.R. Bronze, M.F. Castro, M.H.L. Ribeiro, Design of selective production of sophorolipids by Rhodotorula bogoriensis through nutritional requirements, J. Mol. Recognit. 25 (11) (2012) 630–640, https://doi.org/10.1002/jmr.2188.
[41] I.A. Ribeiro, M.R. Bronze, M.F. Castro, M.H.L. Ribeiro, Sophorolipids: improvement of the selective production by Starmerella bombicola through the design of nutritional requirements, Appl. Microbiol. Biotechnol. 97 (5) (2013) 1875–1887, https://doi.org/10.1007/s00253-012-4437-x.
[42] I.A.C. Ribeiro, C.M.C. Faustino, P.S. Guerreiro, R.F.M. Frade, M.R. Bronze, M. F. Castro, M.H.L. Ribeiro, Development of novel sophorolipids with improved cytotoxic activity toward MDA-MB-231 breast cancer cells, J. Mol. Recognit. 28 (3) (2015) 155–165, https://doi.org/10.1002/jmr.2403.
[43] S.I.C. Ricardo, I.I.L. Anjos, N. Monge, C.M.C. Faustino, I.A.C. Ribeiro, A glance at antimicrobial strategies to prevent catheter-associated medical infections, ACS Infect. Dis. 6 (12) (2020) 3109–3130, https://doi.org/10.1021/acsinfecdis.0c00526.
[44] K. Sambanthamoorthy, X. Feng, R. Patel, S. Patel, C. Paranavitana, Antimicrobial and antibiofilm potential of biosurfactants isolated from lactobacilli against multi-drug-resistant pathogens, BMC Microbiol. 14 (1) (2014) 197, https://doi.org/10.1186/1471-2180-14-197.
[45] S. Satitsri, C. Muanprasat, Chitin and chitosan derivatives as biomaterial resources for biological and biomedical applications, Molecules 25 (24) (2020) 5961, https://doi.org/10.3390/molecules25245961.
[46] V. Shah, D. Badia, P. Ratsep, Sophorolipids having enhanced antibacterial activity, Antimicrob. Agents Chemother. 51 (1) (2007) 397–400, https://doi.org/10.1128/AAC.01118-06.
[47] I. Silvestro, M. Lopreiato, A. Scotto d'Abusco, V. Di Lisio, A. Martinelli, A. Piozzi, I. Francolini, Hyaluronic acid reduces bacterial fouling and promotes fibroblasts' adhesion onto chitosan 2D-wound dressings, Int. J. Mol. Sci. 21 (6) (2020) 2070, https://doi.org/10.3390/ijms21062070.
[48] A. Singh, S.S. Narvi, P.K. Dutta, N.D. Pandey, External stimuli response on a novel chitosan hydrogel crosslinked with formaldehyde, Bull. Mater. Sci. 29 (3) (2006) 233–238, https://doi.org/10.1007/BF02706490.
[49] C. Valotteau, I.M. Banat, C.A. Mitchell, H. Lydon, R. Marchant, F. Babonneau, C.-M. Pradier, N. Baccile, V. Humblot, Antibacterial properties of sophorolipid-modified gold surfaces against Gram positive and Gram negative pathogens, Colloids Surf. B Biointerfaces 157 (2017) 325–334, https://doi.org/10.1016/j.colsurfb.2017.05.072.
[50] D.A. Vaz, E.J. Gudiña, E.J. Alameda, J.A. Teixeira, L.R. Rodrigues, Performance of a biosurfactant produced by a Bacillus subtilis strain isolated from crude oil samples as compared to commercial chemical surfactants, Colloids Surf. B Biointerfaces 89 (2012) 167–174, https://doi.org/10.1016/j.colsurfb.2011.09.009.
[51] Y.-H. Wei, I.-M. Chu, Enhancement of surfactin production in iron-enriched media by bacillus subtilis ATCC 21332, Enzym. Microb. Technol. 22 (8) (1998) 724–728, https://doi.org/10.1016/S0141-0229(98)00016-7.
[52] M. Wlaschek, P. Maity, E. Makrantonaki, K. Scharffetter-Kochanek, Connective tissue and fibroblast senescence in skin aging, J. Investig. Dermatol. 141 (4S) (2021) 985–992, https://doi.org/10.1016/j.jid.2020.11.010.
[53] F. Zamboni, C. Okoroafor, M.P. Ryan, J.T. Pembroke, M. Strozyk, M. Culebras, M. N. Collins, On the bacteriostatic activity of hyaluronic acid composite films, Carbohydr. Polym. 260 (2021), 117803, https://doi.org/10.1016/j.carbpol.2021.117803.
[54] F. Zamboni, C.K. Wong, M.N. Collins, Hyaluronic acid association with bacterial, fungal and viral infections: Can hyaluronic acid be used as an antimicrobial polymer for biomedical and pharmaceutical applications? Bioact. Mater. 19 (2023) 458–473, https://doi.org/10.1016/j.bioactmat.2022.04.023.
[55] X. Zhang, R.D. Ashby, D.K.Y. Solaiman, Y. Liu, X. Fan, Antimicrobial activity and inactivation mechanism of lactonic and free acid sophorolipids against Escherichia coli O157:H7, Biocatal. Agric. Biotechnol. 11 (2017) 176–182, https://doi.org/10.1016/j.bcab.2017.07.002.